LETTER

A Metal Matrix Composite Prepared from Electrospun TiO_2 Nanofibers and an Al 1100 Alloy via Friction Stir Processing

Lifeng Zhang,[†] Ramya Chandrasekar,[†] Jane Y. Howe,[‡] Michael K. West,[†] Nyle E. Hedin,[†] William J. Arbegast,*[,†] and Hao Fong*[,†]

South Dakota School of Mines and Technology, Rapid City, South Dakota 57701, and Materials Science and Technology Division, Oak Ridge National Laboratory, Oak Ridge, Tennessee 37831

ABSTRACT Electrospun TiO_2 nanofibers, consisting of anatase phase TiO_2 single-crystalline crystallites with sizes of ~10 nm, were impregnated into an Al 1100 alloy by the technique of friction stir processing (FSP). The studies of the resulting TiO_2−Al composite revealed that the electrospun TiO_2 nanofibers with diameters of ~200 nm were broken into nanoparticles during FSP; the in situ generated pristine surfaces led to the interfacial reaction between TiO_2 and Al and resulted in the formation of strong interfaces between the electrospun TiO_2 nanoparticles and the Al 1100 matrix. This was evidenced by the fact that the filler−matrix fracture always occurred on the Al matrix side in the interfacial region. Consequently, the TiO_2−Al composite made from the electrospun TiO_2 nanofibers possessed a significantly higher Vickers hardness than that made from a commercially available anatase phase TiO_2 nanopowder, of which the organic and/or carbonaceous contaminants on the surface impeded the interfacial reaction between TiO_2 and Al during FSP.

KEYWORDS: metal matrix composites • friction stir processing • electrospinning • TiO_2 nanofibers

Friction stir processing (FSP) is an emerging technique that can be utilized to modify local microstructures of metals (e.g., Al and Mg) and their alloys. FSP uses the same methodology as friction stir welding, which is a solid-state joining technique invented at the Welding Institute (TWI) in the U.K. approximately 20 years ago for welding aerospace Al alloys that were not able to be joined through the conventional fusion welding method (1, 2). To perform FSP on a metal plate, a specially designed cylindrical tool is stirred at a high speed and plunged into a selected area. The nonconsumable tool has a small-diameter pin with a larger-diameter coaxial shoulder. When the tool approaches the selected area, the stirring pin contacts the surface first and rapidly softens a small column of metal with the generated frictional heat. The shoulder then makes contact with the metal surface, restricting further penetration while generating more frictional heat and causing an intense plastic deformation of a larger cylindrical metal column around the inserted pin. The dynamic recrystallization of metal in the stirred zone results in finer and more homogeneous grain microstructures, which can be controlled by carefully choosing the tool's geometry as well as the processing parameters. Because the microstructural refinement induces superplasticity, FSP is an effective method to tailor and/or improve the surface characteristics as well as mechanical properties of metallic materials (3, 4).

Recently, the development of metal matrix composites with ceramic and/or carbonaceous additives using FSP has been attracting growing attention because the increasing demand for high-performance and lightweight materials in the aerospace and automobile industries as well as for military applications such as protective armors. Inspired by the study reported by Mishra and co-workers (5), where SiC was stirred into Al and the resulting composite showed significantly higher mechanical properties, numerous research efforts have been devoted to the innovative surface and/or bulk metal matrix composites including SiC−Mg (6), carbon nanotubes−Mg (7), SiO_2−Mg (8), ZrO_2−Mg (9), and nitinol−Al (10). Many of these composites showed distinguishably improved surface characteristics and/or mechanical properties; nonetheless, they were exclusively prepared from powders with particle sizes ranging from micrometers to nanometers. Presently, the rapidly developing technique of "electrospinning" provides a straightforward and cost-effective approach to preparing an interesting type of ceramic material termed "nanofibers" with diameters ranging from submicrometers to nanometers and aspect ratios of 1000 or higher. Electrospun ceramic (e.g., SiO_2 and TiO_2) nanofibers are generally prepared by electrospinning spin dopes containing ceramic precursors and carrying polymers followed by high-temperature pyrolysis (11−14). It is an aim of this study to prepare, characterize, and evaluate a metal matrix composite made from this interesting type of ceramic material (specifically the electrospun TiO_2 nanofibers) using the technique of FSP. It is noteworthy that the detailed

* Corresponding authors. Tel: (605) 394-6924 (W.J.A.), (605) 394-1229 (H.F.). Fax: (605) 394-3369 (W.J.A.), (605) 394-1232 (H.F.). E-mail: William.Arbegast@sdsmt.edu (W.J.A.), Hao.Fong@sdsmt.edu (H.F.).

Received for review February 12, 2009 and accepted April 13, 2009

[†] South Dakota School of Mines and Technology.

[‡] Oak Ridge National Laboratory.

DOI: 10.1021/am900095x

© 2009 American Chemical Society

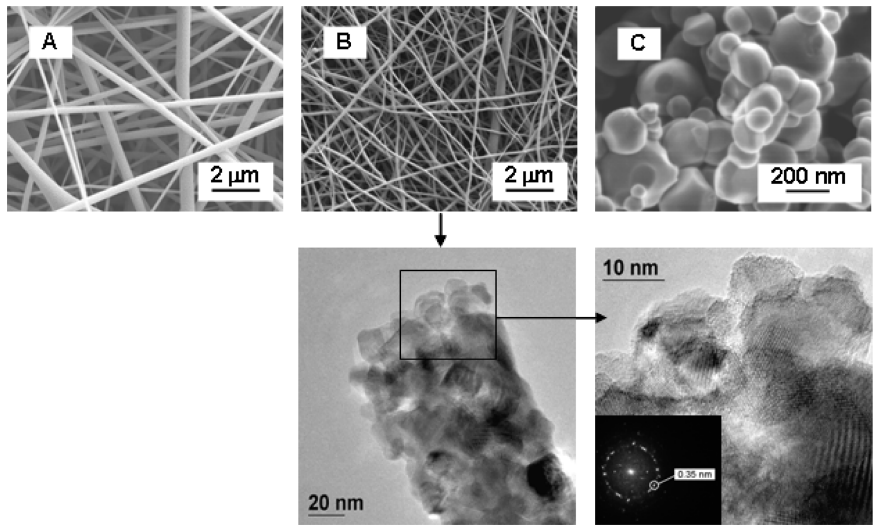

FIGURE 1. Scanning electron microscopy images showing the representative morphologies of (A) the as-electrospun precursor nanofibers containing PVP and TNBT, (B) the final electrospun TiO_2 nanofibers after pyrolysis, and (C) the commercial TiO_2 nanopowder. The HRTEM images (bottom) and the corresponding electron diffraction pattern (inset) confirm that the electrospun TiO_2 nanofibers consisted of anatase phase TiO_2 single-crystalline crystallites with a size of ~10 nm.

physical aspects of FSP have not been fully understood despite the considerable advancement of the technique in the past decade. Previous research suggested that the development of metal matrix composites via FSP was achieved under solid-state conditions, with no interfacial reaction occurring between fillers and matrices during the processing (3); however, no detailed studies of filler−matrix interfaces generated during FSP have been conducted. It is the other aim of this study to investigate the interfaces and the resulting mechanical properties of the metal matrix composites prepared via FSP, specifically the two TiO_2−Al composites prepared from the electrospun TiO_2 nanofibers and a commercially available TiO_2 nanopowder, respectively.

Ramesh and co-workers reported that the impregnation of TiO_2 particles into the Al 6061 alloy could lead to a higher hardness and a lower wear coefficient of the resulting composite (15). In our study reported herein, the Al 1100 alloy was selected because the content/purity of Al in the alloy was high (>99%); it was thus more convenient to investigate and interpret the structures and properties of the resulting TiO_2−Al composites prepared via FSP. High-resolution transmission electron microscopy (HRTEM) was employed to examine the interfacial regions between the TiO_2 fillers and the Al matrices in the composites; additionally, the Vickers hardness of the composites was measured and analyzed.

The electrospun TiO_2 nanofibers were prepared using the procedure developed by our group (16). The spin dope was made by dissolving titanium(IV) *n*-butoxide (TNBT) and poly(vinylpyrrolidone) (PVP) in *N*,*N*-dimethylformamide with a trace amount of acetic acid to control the hydrolysis (gelation) of TNBT. The electrospinning was conducted in an open environment (inside a fume hood) at a room temperature of 25 °C, and the applied voltage was set at 15 kV using a high-voltage power supply (ES30P) purchased from Gamma High Voltage Research Inc. (Ormond Beach, FL). Figure 1A showed the representative morphology of the as-electrospun precursor nanofibers, which had diameters in the range of 50−500 nm. After these precursor nanofibers were placed under ambient conditions for several days to allow the moisture in the air to completely hydrolyze (gel) the TNBT in the fibers, they were then pyrolyzed at 500 °C in air for 6 h to burn/remove the organic components. The final electrospun TiO_2 nanofibers had diameters of ~200 nm, as shown in Figure 1B. The HRTEM images in Figure 1 indicate that the electrospun TiO_2 nanofibers were polycrystalline, and the nanofibers were comprised of anatase phase TiO_2 single-crystalline crystallites with a size of ~10 nm. A commercially available anatase phase TiO_2 nanopowder (Figure 1C) with an average particle size of ~200 nm, purchased from Acros Organics (product number: 21358) through Fisher Scientific Inc. (Pittsburgh, PA), was also studied for comparison.

The electrospun TiO_2 nanofibers (or the commercial TiO_2 nanopowder) were stirred into the Al 1100 alloy by the modified FSP technique of friction stir spot-welding (plunge-type) (17). During processing, holes with a diameter of 0.1 in. and a depth of 0.09 in. were first drilled in an Al 1100 alloy plate with a thickness of 0.125 in.; subsequently, the holes were filled with 9 mg of nanofibers (or nanopowder) and then covered by another Al 1100 plate with the same thickness on the top. This was followed by stirring and plunging of a fixed pin tool through the upper and lower plates, as schematically shown in Figure 2A. The rotational speed of the tool was set at 1400 rpm, while the plunging speed and force were set at 0.3 ipm and 1000 lb, respectively. After the two plates were welded together by the generated frictional heat (Figure 2B), the tool was retracted, leaving a hole in the center of the spot and producing the TiO_2−Al composite in the nugget zone where the nanofibers or nanopowder had been stirred into the Al matrix (Figure 2C). The samples for TEM examination were first cut from the nugget zones and then mechanically ground and ion-milled into thin specimens having the required thickness.

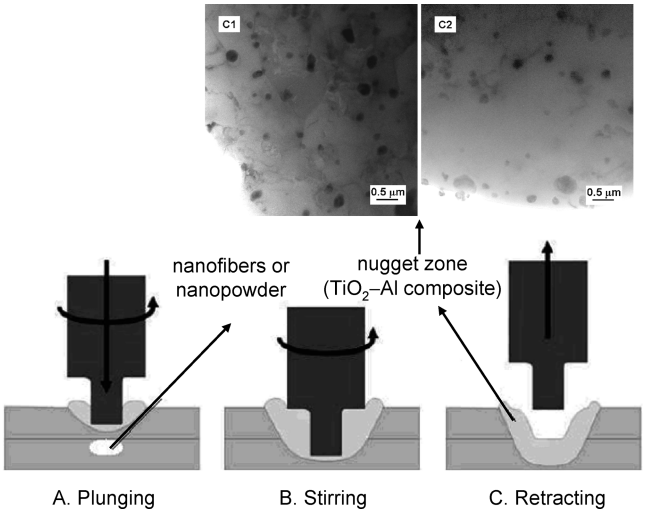

FIGURE 2. Schematic representations of FSP on the electrospun TiO_2 nanofibers or the commercial TiO_2 nanopowder into an Al 1100 alloy and the formation of a nugget zone (TiO_2–Al composite). The TEM images show the representative morphological structures of the TiO_2–Al composites made from the nanofibers (C1) and the nanopowder (C2).

To remove organic contaminants on the surface, all specimens were treated in an E. A. Fischione Plasma Cleaner prior to TEM examination. The HRTEM images indicated that both the nanofibers and the nanopowder in the prepared TiO_2–Al composites primarily existed as nanoparticles with sizes ranging from tens to hundreds of nanometers (images C1 and C2 in Figure 2). The electrospun TiO_2 nanofibers were broken into nanoparticles because of the strong shear stress associated with FSP. It appeared that most electrospun TiO_2 nanoparticles within the composite consisted of multiple grains, despite the fact that some completely separated, single-crystalline grains could occasionally be found. Figure 3 is a representative HRTEM image showing the interfacial region between an electrospun TiO_2 nanoparticle and the surrounding Al matrix. Energy-dispersive X-ray spectroscopy (EDS) along with TEM was employed to analyze the elemental compositions at different locations. In a typical EDS examination of an electrospun TiO_2 nanoparticle, the high Al concentration was identified at spot A (Figure 3A), which was located at the boundary of the TiO_2 particle. The Al concentrations at spots B–D (Figure 3B–D), with locations gradually away from the boundary, were significantly lower. It is noteworthy that the differences of the Al concentrations between spot A and spots B–D were quite large, whereas those among spots B–D were relatively small. This suggested an interfacial reaction instead of a bulk reaction occurred between the Al matrix and the electrospun TiO_2 nanoparticle during FSP. To further study the interface and eliminate the influence of the Al matrix in the EDS results, several TiO_2 nanoparticles that were partially protruded from the Al matrix in the TiO_2–Al composites prepared from either the electrospun TiO_2 nanofibers or the commercial TiO_2 nanopowder were identified and examined. The protruded electrospun TiO_2 nanoparticles showed consistent EDS results at different locations on the boundary where Al was the overwhelming component (Figure 4A–C, top). On the other hand, the protruded TiO_2 nanoparticles from the commercial nanopowder showed different EDS results at different locations on the boundary; i.e., Al was the overwhelming component at some locations, while both Al and Ti were significant components at other locations (Figure 4A–C, bottom). These results suggested that the electrospun TiO_2 nanoparticles formed relatively strong interfaces with the matrix in the composite and the filler–matrix fracture always occurred on the Al matrix side in the interfacial region; in contrast, the commercial TiO_2 nanoparticles formed relatively weak interfaces and the fracture could occur in either the filler or the matrix side in the interfacial region. It was our speculation that the thickness of the interfaces, if there was any, in the TiO_2–Al composite prepared from the nanopowder was significantly thinner than that prepared from the nanofibers.

The processing temperature during FSP was in the range of 300–500 °C for Al alloys (18, 19), which was well below the melting point of Al (660 °C). According to the Ellingham diagram for the reduction reactions of metal oxides (20), the Al/Al_2O_3 line is under the Ti/TiO_2 line when the temperature is below 600 °C. This indicates that the Gibbs free energy of the reaction between Al and TiO_2 at the FSP processing temperature is negative; i.e., the reaction is spontaneous and/or favorable. In the meantime, our study showed that the reaction only occurred in the interface, and this was because both Al and TiO_2 (melting point: 1855 °C) were in the solid state at the FSP processing temperature. Similar results were reported by Chen and co-workers (21): they prepared TiO_2 films on Al substrates by dip-coating followed by pyrolysis at 450 °C; their results indicated that Al diffuses into TiO_2 and Al_2O_3 was found at the boundary between Al and TiO_2. It is noteworthy that the lack of reaction evidence between TiO_2 and Al during FSP from X-ray diffraction analysis in a previous report (22) is probably due to the fact that the reaction only occurs at the interface; therefore, the resulting product of Al_2O_3 can only be detected by direct examination of the interface like what we did in this study.

When the two TiO_2–Al composites are compared, it was found that the interfacial differences resulted from the surface discrepancies of the impregnated TiO_2 nanoparticles in the composites. For the composite made from the electrospun TiO_2 nanofibers, the in situ generated TiO_2 fresh surface was pristine and superhydrophilic (water contact angle close to 0°) (23). The interfacial reaction between Al and TiO_2 could readily occur. On the contrary, the surface of the commercial TiO_2 nanopowder was contaminated by organic substances; this was because TiO_2 had a high tendency to adsorb organic substances in air, as evidenced by the recent reports on the mechanism of UV-induced superhydrophilicity on TiO_2 surfaces (24, 25). The presence of organic and/or carbonaceous contaminants on the surface of TiO_2 impeded the interfacial reaction between Al and TiO_2. This is because carbon cannot reduce TiO_2 in the FSP processing temperature range according to the Ellingham diagram (20), in which both C/CO and C/CO_2 lines lie above the Ti/TiO_2 line at the temperature below 600 °C. The

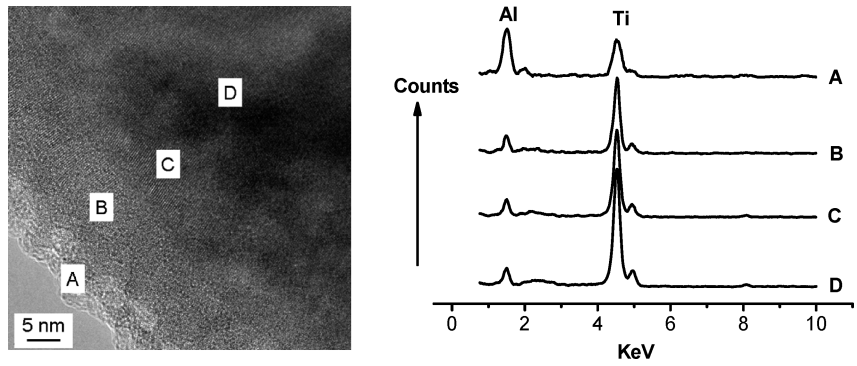

FIGURE 3. Representative HRTEM image showing an electrospun TiO_2 nanoparticle in the TiO_2–Al composite and EDS examinations of the elemental compositions at four locations (A–D).

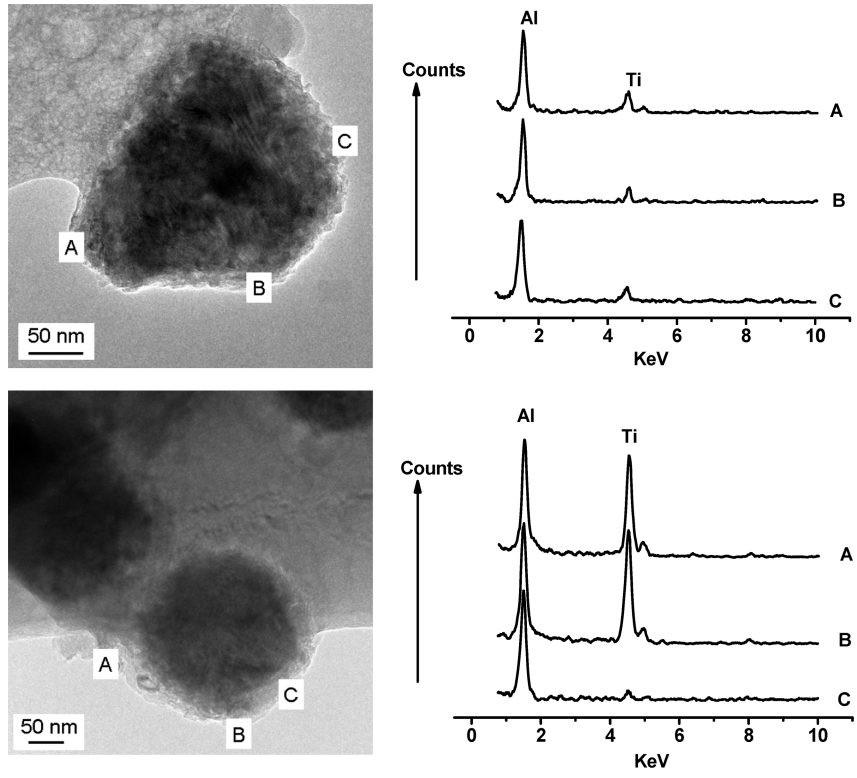

FIGURE 4. Representative TEM images showing two protruded TiO_2 nanoparticles from the electrospun TiO_2 nanofibers (top) and the commercial TiO_2 nanopowder (bottom) in the TiO_2–Al composites and the respective EDS examinations of the elemental compositions at three locations (A–C) in each composite.

occurrence of an interfacial reaction between the Al matrix and the electrospun TiO_2 nanoparticles resulted in the formation of an interface, which was much stronger than that between the Al matrix and the commercial TiO_2 nanoparticles. This was supported by the fact that the filler–matrix fracture always occurred on the Al matrix side in the interfacial region for the composite containing electrospun TiO_2 nanoparticles, while the fracture could occur in either the filler or the matrix side in the interfacial region for the composite containing commercial TiO_2 nanoparticles (Figure 4).

The microhardness test revealed that the TiO_2–Al composite prepared from the electrospun TiO_2 nanofibers possessed a significantly higher Vickers hardness than the composite prepared from the commercial TiO_2 nanopowder (Figure 5), confirming a stronger interface between the Al matrix and the electrospun TiO_2 nanoparticles. Because TiO_2 was filled in a drilled hole for FSP, the mixing of TiO_2 and Al only happened in the nugget zone (Figure 2). Because no TiO_2 was beyond the nugget boundary, the hardness of both composites had similar values outside the nugget zone. Because of the fact that the drilled hole was much smaller than the final nugget zone, there was an expected gradient of the TiO_2 concentration from the nugget boundary, resulting in the hardness variation as a function of the distance from the nugget boundary. It is noteworthy that several parallel experiments were carried out during this study, and the profile as shown in Figure 5 was representative. The preparation and evaluation of the samples in each of the parallel experiments were carried out under exactly the same conditions. The reason that there was no standard deviation included in Figure 5 was because the actual distances of the measuring spots (from the nugget bound-

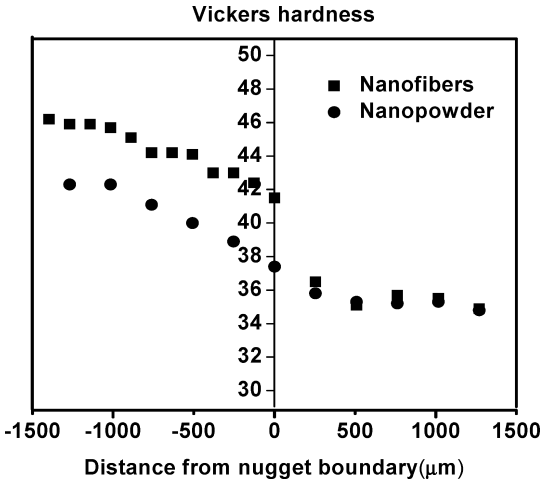

FIGURE 5. Variations of the Vickers hardness in the two TiO_2−Al composites made from the electrospun TiO_2 nanofibers (■) and the commercial TiO_2 nanopowder (●).

aries) for the microhardness tests were not exactly the same in each of the parallel experiments.

In summary, this research has demonstrated that an interesting type of ceramic material (i.e., electrospun TiO_2 nanofibers) can be utilized for the development of metal matrix composites via FSP. The prepared electrospun TiO_2 nanofibers with diameters of ~200 nm were polycrystalline and consisted of anatase phase TiO_2 single-crystalline crystallites with a size of ~10 nm. When the electrospun TiO_2 nanofibers were stirred into an Al 1100 alloy, the strong shear stress associated with FSP tended to break the nanofibers into nanoparticles with sizes ranging from tens to hundreds of nanometers, and the in situ generated pristine surfaces of TiO_2 facilitated the interfacial reaction between Al and TiO_2 and further resulted in the formation of strong interfaces between the electrospun TiO_2 nanoparticles and the Al matrix in the TiO_2−Al composite, as evidenced by the filler−matrix fracture always occurring on the Al matrix side in the interfacial region. In contrast, the TiO_2−Al composite made from a commercially available anatase phase TiO_2 nanopowder with particle sizes ranging from tens to hundreds of nanometers formed relatively weak interfaces because of the presence of organic and/or carbonaceous contaminants on the TiO_2 surface, which impeded the reaction between Al and TiO_2, and the filler−matrix fracture could occur in either the filler or the matrix side in the interfacial region. Consequently, the TiO_2−Al composite made from the electrospun TiO_2 nanofibers possessed a significantly higher Vickers hardness than the control sample that was made from the commercial TiO_2 nanopowder. Collectively, not only did this research improve the fundamental understanding of the FSP technique as well as the microstructures and properties in the resulting metal matrix composites but also the study suggested that the innovative materials of electrospun ceramic nanofibers could play an important role in the development of novel metal matrix composites with desired surface characteristics and/or mechanical properties.

Acknowledgment. This research was supported by the U.S. Air Force Research Laboratory under the Cooperative Agreement Number FA9453-06-C-0366. The HRTEM study was sponsored by the U.S. Department of Energy, the Assistant Secretary for Energy Efficiency & Renewable Energy, Office of FreedomCAR and Vehicle Technologies, through the High Temperature Materials Laboratory User Center at the Oak Ridge National Laboratory.

REFERENCES AND NOTES

(1) Thomas, W. M.; Nicholas, E. D.; Needham, J. C.; Murch, M. G.; Temple-Smith, P.; Dawes, C. J. U.S. Patent 5,460,317, 1995.
(2) Arbegast, W. J. *Weld. J.* **2006**, *85* (3), 28–35.
(3) Ma, Z. Y. *Metall. Mater. Trans. A* **2008**, *39* (3), 642–658.
(4) Mishra, R. S.; Ma, Z. Y. *Mater. Sci. Eng., R* **2005**, *50* (1−2), 1–78.
(5) Mishra, R. S.; Ma, Z. Y.; Charit, I. *Mater. Sci. Eng., A* **2003**, *341* (1−2), 307–310.
(6) Morisada, Y.; Fujii, H.; Nagaoka, T.; Fukusumi, M. *Mater. Sci. Eng., A* **2006**, *433* (1−2), 50–54.
(7) Morisada, Y.; Fujii, H.; Nagaoka, T.; Fukusumi, M. *Mater. Sci. Eng., A* **2006**, *419* (1−2), 344–348.
(8) Lee, C. J.; Huang, J. C.; Hsieh, P. J. *Scr. Mater.* **2006**, *54* (7), 1415–1420.
(9) Chang, C. I.; Wang, Y. N.; Pei, H. R.; Lee, C. J.; Huang, J. C. *Mater. Trans.* **2006**, *47* (12), 2942–2949.
(10) Dixit, M.; Newkirk, J. W.; Mishra, R. S. *Scr. Mater.* **2007**, *56* (6), 541–544.
(11) Dzenis, Y. *Science* **2004**, *304* (5679), 1917–1919.
(12) Li, D.; Xia, Y. *Adv. Mater.* **2004**, *16* (14), 1151–1170.
(13) Li, D.; Xia, Y. *Nano Lett.* **2004**, *4* (5), 933–938.
(14) Greiner, A.; Wendorff, J. H. *Angew. Chem., Int. Ed.* **2007**, *46* (30), 5670–5703.
(15) Ramesh, C. S.; Anwar Khan, A. R.; Ravikumar, N.; Savanprabhu, P. *Wear* **2005**, *259* (1−6), 602–608.
(16) Chandrasekar, R.; Zhang, L.; Howe, J. Y.; Hedin, N. E.; Zhang, Y.; Fong, H. *J. Mater. Sci.* **2009**, *44* (5), 1198–1205.
(17) Kalagara, S.; Muci-Kuchler, K. In *Friction Stir Welding and Processing IV*; Mishra, R. S., Mahoney, M. W., Lienert, T. J., Jata, K. V. Eds.; The Minerals, Metals & Materials Society: Warrendale, PA, 2007; Session V, pp 369−378.
(18) Schneider, J. A. In *Friction Stir Welding and Processing*; Mishra, R. S., Mahoney, M. W. Eds.; ASM International: Materials Park, OH, 2007; Chapter 3, pp 37−49.
(19) Woo, W.; Feng, Z.; Wang, X. L.; Brown, D. W.; Clausen, B.; An, K.; Choo, H.; Hubbard, C. R.; David, S. A. *Sci. Technol. Weld. Joining* **2007**, *12* (4), 298–303.
(20) Atkins, P.; Overton, T.; Rourke, J.; Weller, M.; Armstrong, F. *Shriver & Atkins Inorganic Chemistry*, 4th ed.; W. H. Freeman and Co.: New York, 2006; Chapter 5, p 163.
(21) Chen, S. Z.; Zhang, P. Y.; Zhu, W. P.; Chen, L.; Xu, S. M. *Appl. Surf. Sci.* **2006**, *252* (20), 7532–7538.
(22) Howard, S. M.; Jasthi, B. K.; Arbegast, W. J.; Grant, G. J.; Herling, D. R. In *Friction Stir Welding and Processing III*; Jata, K. V., Mahoney, M. W., Mishra, R. S. Eds.; The Minerals, Metals & Materials Society: Warrendale, PA, 2005; Session III, p 139.
(23) Wang, Y.; Wang, H.; Yan, F. *Surf. Interface Anal.* **2009**, DOI 10.1002/sia.3039.
(24) Zubkov, T.; Stahl, D.; Thompson, T. L.; Panayotov, D.; Diwald, O.; Yates, J. T. *J. Phys. Chem. B* **2005**, *109* (32), 15454–15462.
(25) Thompson, T. L.; Yates, J. T. *Chem. Rev.* **2006**, *106* (10), 4428–4453.

AM900095X